

# Optimum Design of Die Casting Plunger Tip Considering Air Entrainment

T. Yoshimura\*, K. Yano, T. Fukui, S. Yamamoto, S. Nishido, M. Watanabe and Y. Nemoto

*Faculty of Engineering, Gifu University, Gifu City, Japan  
AISIN TAKAOKA CO., LTD., Toyota City, Japan  
TERRABYTE CO., LTD., Bnkyo-ku, Japan*

Die casting is used for the manufacture of various products. Die casting is suitable for mass production and has the advantage of being able to accurately fashion objects of complicated shapes. One disadvantage of die casting for high-speed injection molding is the occurrence of blow holes.

To avoid the occurrence of blow holes, shaped plunger tips is very effective in actual manufacturing facilities. In this paper, fluid behavior and the quantity of air entrainment caused by the movement of a die-cast plunger in a sleeve and by the tip's shape are analyzed using a CFD simulator. The optimum shape of the die-cast plunger tip for reducing the amount of entrained air and preventing the occurrence of blow holes in die-cast products is calculated. An optimization is performed utilizing the simplex method incorporating a CFD simulator. The effectiveness of the proposed system is demonstrated through CFD simulations and experiments in actual manufacturing facilities.

**Keywords:** Die casting, CFD simulator, Optimization, Process control

## 1 Introduction

Die casting is used for the manufacture of various products including automobiles. Die casting is suitable for mass production and has the advantage of being able to accurately fashion objects of complicated shapes. Furthermore, as a smooth casting surface is obtained, further mechanical work is not required and materials are conserved, in contrast with the case using sand casting methods. One disadvantage of die casting for high-speed injection molding is the occurrence of blow holes.

To avoid the occurrence of blow holes, shaped plunger tips is very effective in actual manufacturing facilities. For the typical shape of plunger tip the flat type are used in actual manufacturing facilities. The cast products look good cosmetically. However, expansion of compressed air by blister test reveals the existence of internal defects such as those seen in Fig. 1. The result is several big bulges in various parts.

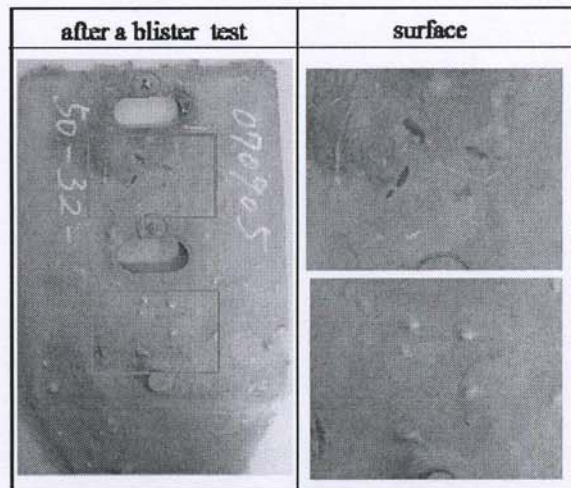


**Fig. 1 Product after blister test-An examination to investigate the quantity of air entrainment by heating up a test piece to near the melting point in a furnace and inflating**

Many studies of the defects of die casting have been performed.<sup>1-4</sup> Recently, a method that automatically optimizes injection pattern has been developed to reduce air entrainment.<sup>5,6</sup> However, the injection velocity and shape of the runner are the most common point of such studies. The only study looking at the shape of the plunger tip is one study using shape such as a snowplow and farmer tools for Cold Flakes; therefore, there are many aspects of the plunger tip's effects in the system which still have not been elucidated, especially, the occurrence of blow holes.

In this paper, fluid behavior and the quantity of air entrainment caused by a die-cast plunger movement in a sleeve are analyzed using a CFD (Computational Fluid Dynamics) simulator. This clarifies the mechanism of air entrainment by the plunger tip. The goal was to optimize the design to reduce air entrainment and prevent the occurrence of blow holes in die-cast products. The optimization was performed by the simplex method incorporating a CFD simulator (FLOW-3D). The



effectiveness of the proposed system is demonstrated through CFD simulations and experiments in actual manufacturing facilities.

## 2 Defect Analysis by CFD Simulator

### 2.1 CFD Simulator and Simulation Condition

In this study, the fluid analysis software, FLOW-3D (FlowScience Inc.) is used. This simulator is a fluid-calculation software that analyzes three-dimensional transient flows of compressible/incompressible viscous fluids, and can treat free surfaces. The free surface calculation is performed based on the Volume of Fluid (VOF) method.<sup>7</sup> The Fractional Area Volume Obstacle Representation (FAVOR) method is used for the shape matching of a complicated obstacle.<sup>8</sup> The validity of this simulator has been demonstrated in many studies.<sup>9</sup>

A die for test parts whose thickness is 0.005 m was used, and a sleeve whose bore is 0.075 m and length is 0.44 m was used. The constitution of the die and sleeve and the mesh setting depicting the simulation field are shown in Fig. 2. In this simulation, the die parts were not considered. Normally, running simulation of all parts, from sleeve to product, is best for in-depth analysis in a wide sphere. However, this was impractical because it would have required an inordinate amount of time, especially for optimization.

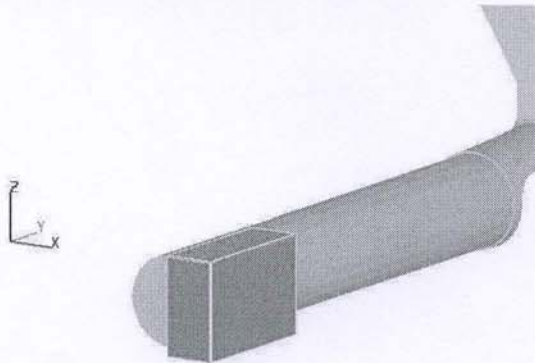


**Fig. 2 Setting mesh a block for CFD simulation**

As a target molten metal and casting mold, an aluminum alloy (ADC12) was applied in 460 cc and hot work tool steel (SKD61) was assumed. In the simulation, the viscosity, solidification and heat conduction were considered. Table 1 shows physical parameters of the molten metal. The injection velocity was set at  $0.5 \text{ m}\cdot\text{s}^{-1}$ .

**Table 1 Fluid properties of ADC12.**

Density of fluid	2700[ $\text{kg}\cdot\text{m}^{-3}$ ]
Viscosity of fluid	0.0030[ $\text{Pa}\cdot\text{s}$ ]
Specific heat	1100[ $\text{J}\cdot\text{kg}^{-1}\text{K}^{-1}$ ]
Thermal Conductivity	100.5[ $\text{W}\cdot\text{m}^{-1}\text{K}^{-1}$ ]
Initial temperature	953.15[K]

### 2.2 Evaluation of Air Entrainment

The quantity of air entrainment is a key indicator in the casting field, but it is difficult to measure experimentally. In this paper, therefore, it is estimated using a CFD simulator.

In this simulator, air entrainment at the liquid surface is based on the concept that turbulent eddies raise small liquid elements above the free surface that may trap air and carry it back into the body of the liquid. The extent to which liquid elements can be lifted above the free surface depends on whether or not the intensity of the turbulence is enough to overcome the surface-stabilizing forces of gravity and surface tension.<sup>7</sup>

Turbulence transport models characterize turbulence by a specific turbulent kinetic energy  $Q$  and a dissipation function  $D$ . The characteristic size of turbulence eddies is then given by (1).

$$L = 0.1 \frac{\sqrt{Q^3}}{D} \quad (1)$$

This scale is used to characterize surface disturbances. The disturbance kinetic energy per unit volume (i.e., pressure) associated with a fluid element raised to a height  $L$ , and with surface tension energy based on a curvature of  $L$  is given by (2).

$$P_d = \rho g L + \sigma / L \quad (2)$$

where  $\rho$  is the liquid density,  $\sigma$  is the coefficient of surface tension, and  $g$  is the component of gravity normal to the free surface. In addition, because potential energy is the dominant parameter than surface tension in  $P_d$ , It's conceivable that influences of surface tension is small. For air entrainment to occur, the turbulent kinetic energy per unit volume,  $P_t = \rho Q$ , must be larger than  $P_d$ ; i.e., the turbulent disturbances must be large enough to overcome the surface stabilizing forces. The volume of air entrained per unit time,  $V_a$ , is given as (3).

$$\frac{\partial V_a}{\partial t} + u \nabla V_a = R(1 - V_a) \quad (3)$$

where  $R = C_{air} \sqrt{2(P_t - P_d) / \rho}$ ,  $u$  is fluid velocity,  $t$  is



time, and  $C_{air}$  is a coefficient of proportionality:  $C_{air}=0.5$  in this study ; i.e., assume on average that air will be trapped over about half the surface area. If  $P_i$  is less than  $P_d$  then  $V_a$  is zero.

The air entrainment is expressed in (4).

$$A = \sum_{k=1}^n V_{ak} F_{fk} V_{fk} V_{ck} \quad (4)$$

where  $A$  is the quantity of air entrainment,  $V_a$  is the volume of air entrained per unit time,  $F_f$  is the fluid fraction,  $V_f$  is the volume fraction,  $V_c$  is the volume of the mesh cell, and  $n$  is the aggregate number of mesh cells. In this study, the calculated air entrainment is used as measure of evaluation.

### 2.3 Analysis of air entrainment for changing plunger-tip

Simulations of fluid analysis using the general flat tip shown in Fig. 3 were run, and the phenomenon of air entrainment was analyzed. The tip was 0.075 m across. Mesh parameters of analysis are shown in Table 2.

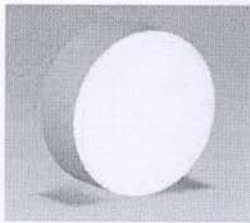


Fig. 3 Flat tip

Table 2 Mesh Parameters.

Block	Cell size [m]	Number of cell
X-direction	0.0005	80
Y-direction	0.0005	240
Z-direction	0.0005	160
Total number of cell		3,072,000

Fig. 4 shows the simulation result with a flat tip. The computational time is about 38 hours by using a PC with a Pentium D 3.4GHz processor.

The simulation result shows clearly that some air is entrained from outside. The reason is that pressed fluid deforms and causes waves although the fluid only rises in the early phase. The quantity of entrained air at 0.1 s is  $A = 0.031$ . In the next section, this study optimizes tip with the immediate goal of minimising the amount of air at the beginning of the injection.

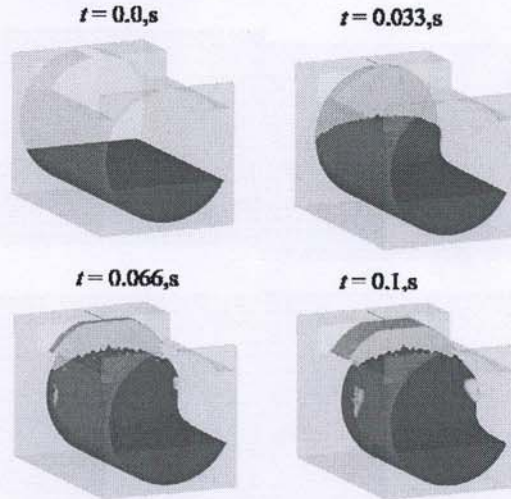
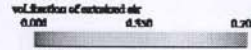


Fig. 4 Simulation result with flat tip

## 3 Optimum Design of Plunger Tip

### 3.1 Formulation of optimization problem

From the results of the foregoing section, a tip designed to decrease the entrained air when the plunger injected by avoiding the formation of a deforming wave is imagined. The idea was to investigate a tip with a curved rather than linear shape, as shown in Fig. 5.

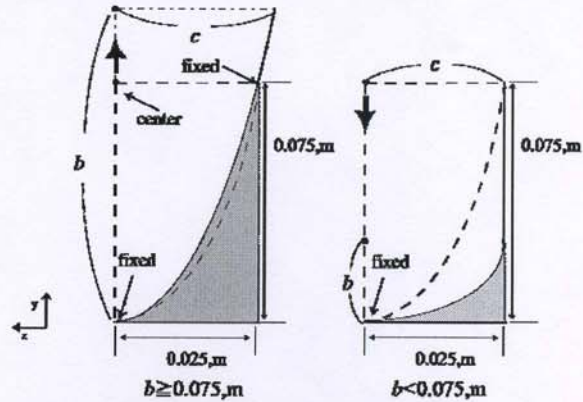


Fig. 5 Concept of optimum tip design: a two-dimensional diagram

In concrete descriptions, the three-dimensional shape can be explained as follows: the direction of injection is the y-direction and the direction normal to it is the z-direction. Then, an elliptical function is represented

$$\frac{x^2}{a^2} + \frac{y^2}{b^2} + \frac{z^2}{c^2} - 1 = 0 \quad (5)$$

where  $a$  of the x-direction and  $b$  of the y-direction are unknown parameters, and  $c$  is depends on  $b$ , as  $c = 0.025$  in  $b < 0.075$  or as (7) in  $b \geq 0.075$ . This



function is used to cut the shape lengthened the head of flat tip 0.025 m.

$$c = 1/\sqrt{(1 - \frac{0.075^2}{b^2})}/0.025^2 \quad (6)$$

Finally, the constrained optimization problem forms equation (8) in which the cost function is the amount of entrained air  $A$  caused at 0.1 s, and  $J_p$  is the penalty term expressed in (9).

$$\begin{aligned} \text{Minimize } J &= A(a,b) + J_p \\ \text{Subject to } a &\geq 0 \end{aligned} \quad (7)$$

$$\begin{aligned} b &\geq 0 \\ x, y, z &\in \mathbb{R}^n \end{aligned}$$

$$J_p = w_1 + w_2 + \dots + w_i \quad (8)$$

where  $w_i$  is the penalty. Each time the penalty conditions hold, the penalty  $w_i = 10^8$ , which is large enough to avoid the penalty conditions, will be added to the point for not to be negative.

An exhaustive search takes time regardless of the setting. Therefore, the simplex method of optimization method was applied to the present problem, where the reflection coefficient  $\alpha = 1.0$ , the expansion coefficient  $\beta = 0.5$ , and the contraction coefficient  $\gamma = 2.0$ . The initial simplex values were  $a = (2, 0.1, 0.02)$  and  $b = (0.05, 0.075, 0.02)$ , and the amount of air  $A$  was  $(0.033, 0.0085, 0.0382)$

### 3.2 Verification by optimum design and simulation

**Table 3 Mesh Parameters.**

Block	Cell size [m]	Number of cell
X-direction	0.0016	35
Y-direction	0.0016	300
Z-direction	0.0016	55
Total number of cell		577,500

Mesh parameter when optimization is shown in Table4. To shorten the amount of computation time the cell size is larger than in the foregoing section (one hour per simulation). Although this changes the conditions of the simulation, the relative relationship is not influenced. The result of a flat tip under the same conditions is  $A = 0.0272$ .

The results of optimization are shown in Fig. 6. The computation time was about 44 hours using a PC with a Pentium D 3.4GHz processor. Consequently, the solutions converged after 19 executions. The obtained optimum shape is shown in Fig. 7:  $a = 16.320$  m,  $b = 0.062$  m. The calculated result for the amount of air entrainment was  $A=0.0016$ .

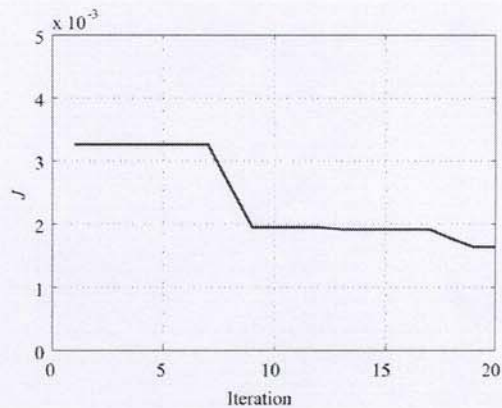


**Fig. 6 Optimization result**

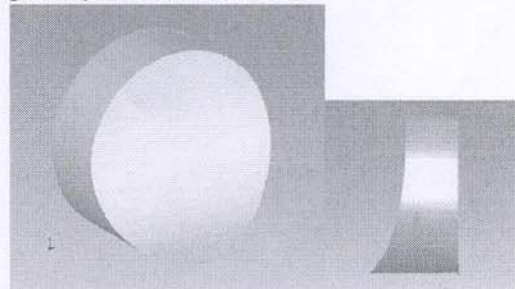


**Fig. 7 Optimum tip shape**

Next, simulation using the optimum tip with the conditions of the foregoing section was measured with a higher-accuracy method. Fig. 9 is the simulation result with the optimum tip shape. The collecting fluid in the center decreases the waves on the sides. As a result, in comparison to Fig. 4, the entrained air is seen to be greatly reduced. The amount of air is  $A = 0.003$ . The result using the optimum tip shape is 90.3 percent lower than that of the conventional flat tip.

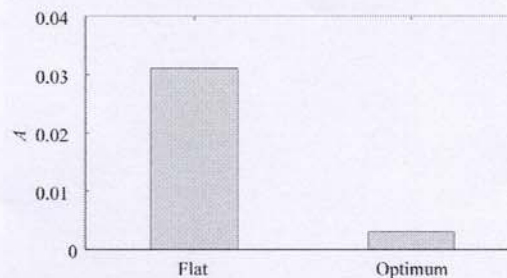


**Fig. 8 Air amount of flat tip vs. optimum tip**



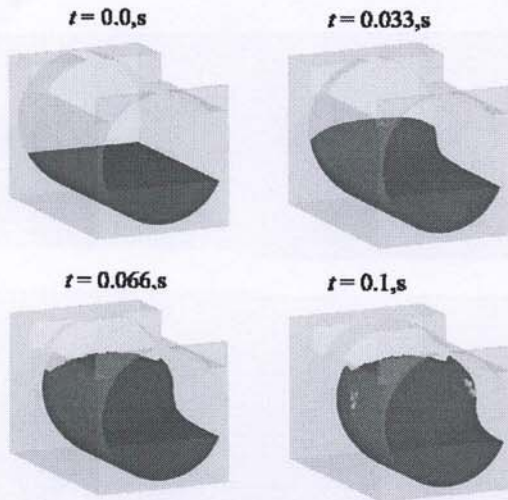


Fig. 9 Simulation result using the optimum tip shape

#### 4 Experimental Results

Experiments for an actual die casting plant were performed with the obtained optimum tip shape. The plunger velocity used in the experiment is shown in Fig. 10 and the result of the blister examination is shown in Fig. 11. In addition, the total area of the air bubble that appeared on the test piece surface after the blister examination is shown in Fig. 12.

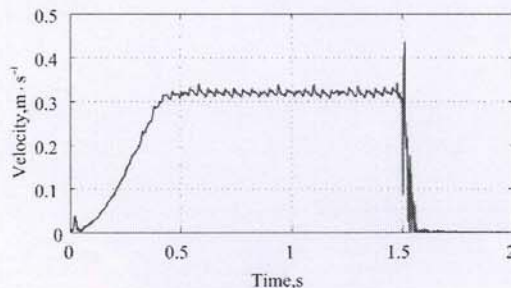


Fig. 10 Experimental velocity

From the results of the blister examination shown in Fig. 11 and Fig. 12, the proposed shape yields fewer air bubbles on the surface compared with the flat shape. Although a big bulge remains in the product, this bulge is caused by the movement of the plunger, not by the shape of tip, and can be reduced by optimizing the velocity. Therefore, combining the optimum plunger tip and an optimum velocity input makes it possible to produce castings without air entrapment.

#### 5 Conclusions

In the present study, fluid simulations considering air entrainment are performed, and the influence of the plunger tip is investigated. By optimizing the design of the plunger tip based on the idea of avoiding the formation of deforming waves. A decrease in the amount of air was achieved. The effectiveness of the tip was demonstrated by experiments in actual casting plants. This tip would be particularly effective in machines not having injection velocity.

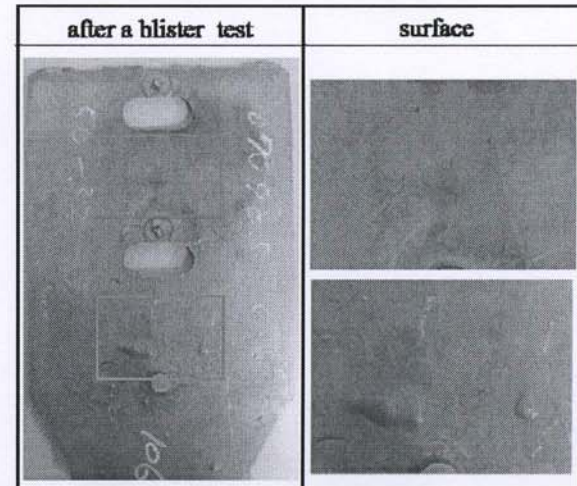


Fig. 11 Results of blister test

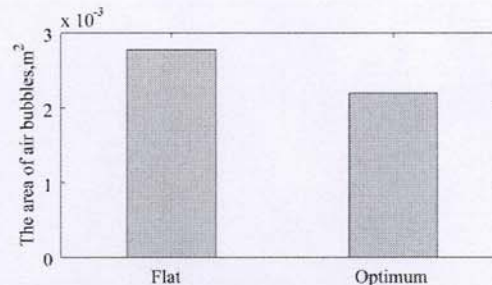


Fig. 12 Areas of air bubbles

#### References

- S. Tanikawa, K. Asai, Y Yang, H Nomura and E Kato: *J. JFS*, Vol. 77, 2005 3, 161-166.
- Marilyn Thome. and Jerald R. Brevick: *North American Die Casting Association*, 2-5, 1995, 53-59
- C.Bdini, F.Bonollo, M.P.Cavatorta, GM La Vecchia, A.Panvini, A.Pola, W.Nicodemi, M.Vedani: *METALLURGICAL SCIENCE AND TECHNOLOGY*, Vol.20, (2002)
- F. Faura, J. Lopez, J. Hernandez: *International Journal of Machine Tools & Manufacture*, Vol. 41, 2001, 173-191
- I.Takahashi, K. Okamoto, S. Sekiyama and Y. Yamagata: *jscs*, Vol.5, (2000)
- I.Takahashi, K.Anzai: *JDCA*, (2007)
- C.W.Hirt, B.D.Nichols : *Journal of Computational Physics*, 39(1981)201
- C.W.Hirt, J.M.Sicilian : *Proc. of 4 th International Conference on Ship Hydrodynamics*, (1985)

M.R.Barkhudarov, S.B.Chin : International Journal  
for Numerical Methods in Fluids, 19, (1994)  
K.Kawamo, M.Yokoyama, T.Iwamoto  
'Fundamentals and Applications of Optimization  
Theory', 2000  
Flow-3D, FlowSciense inc.,  
<http://www.flow3d.com>